

# Nanostructural evolution of Al<sub>3</sub>Sc precipitates in an Al–Sc–Mg alloy by three-dimensional atom probe microscopy

Emmanuelle A. Marquis\* and David N. Seidman

Materials Science and Engineering Department, Northwestern University, Evanston, IL 60208-3108, USA

Received 11 July 2002; Revised 18 June 2003

The effects of Mg alloying on the precipitation of Al<sub>3</sub>Sc precipitates were investigated, focusing on nanostructural evolution during isothermal aging at 300 °C. Three-dimensional atom probe microscopy was performed on samples both in the as-quenched state and after aging for various times. Magnesium tends to segregate at the coherent Al/Al<sub>3</sub>Sc interface, with a measured value of  $1.9 \pm 0.5$  atom nm<sup>-2</sup> for the relative Gibbsian excess of Mg with respect to Al and Sc. This value is constant for all heat treatments, thereby demonstrating that the system is in global thermodynamic equilibrium. This study provides direct experimental evidence for first-principles calculations, which explain morphological changes of Al<sub>3</sub>Sc precipitates in the presence of Mg observed by high-resolution electron microscopy. Evidence for the presence of Mg atoms in the center of the precipitates is also found, and is discussed in terms of heterogeneous nucleation of the precipitates on Mg–Sc atomic clusters. Copyright © 2004 John Wiley & Sons, Ltd.

**KEYWORDS:** atom probe microscopy; Mg segregation; coherent heterophase interface; Gibbsian excess

## INTRODUCTION

Despite its very low solid solubility in aluminum, scandium contributes significantly to improving the strength of Al alloys, having the highest strengthening effect on a per atom basis.<sup>1</sup> Even though the slow coarsening kinetics of the Al<sub>3</sub>Sc precipitates places these alloys as potential candidates for high-temperature applications,<sup>2</sup> the strength of the binary Al–Sc alloys is not sufficient for structural applications, and magnesium alloying not only provides additional solid-solution hardening but also corrosion resistance.<sup>3</sup> Studying the effects of Mg additions on Al<sub>3</sub>Sc precipitation in Al–Sc alloys is therefore important for optimizing the mechanical properties of these multicomponent alloys. From a theoretical viewpoint, addition of Mg to the  $\alpha$ -Al/Al<sub>3</sub>Sc system, where Mg is in solid solution in the  $\alpha$ -Al matrix, constitutes a simple and well-defined system for studying heterophase segregation. Very few detailed and quantitative results on heterophase segregation phenomena in the solid state have been obtained, and the Al–Mg–Sc system brings new insight into the driving forces for segregation of solute species at a coherent heterophase interface.

Atom probe field ion microscopy provides quantitative chemical information of an analyzed specimen on an atom-by-atom basis, and is complementary to high-resolution

electron microscopy (HREM) and small-angle x-ray scattering experiments for the study of complex precipitation processes in aluminum alloys. The atomic-scale resolution of this technique makes it uniquely suited to examine the effects of microalloying and of solute interactions, as demonstrated by the results obtained by Ringer *et al.* employing three-dimensional atom probe (3DAP) microscopy on precipitation processes in aluminum alloys.<sup>4</sup>

The research reported herein follows our initial results obtained by HREM, showing that Mg additions alter the morphology of Al<sub>3</sub>Sc precipitates, i.e. the {100} and {110} facets disappear and the precipitates become spheroidal. Asta *et al.* recently published first-principles calculations demonstrating significant Mg segregation at coherent {100} Al/Al<sub>3</sub>Sc interfaces, where the driving force is electronic in nature.<sup>5</sup> The effects of Mg alloying on the precipitation of Al<sub>3</sub>Sc precipitates are investigated, with this study focusing on the nanostructural evolution during isothermal aging at 300 °C.

## EXPERIMENTAL

### Specimen preparations

A cast Al–2 wt.% Mg–0.2 wt.% Sc alloy was annealed at 618 °C in air for 24 h (to ensure uniformity of the Mg concentration throughout the material), quenched into cold water and then aged in air at 300 °C for 0.33–1040 h. High-resolution electron and three-dimensional atom probe microscopies were performed on samples taken at different aging states. Transmission electron microscopy samples

\*Correspondence to: Emmanuelle A. Marquis, Sandia National Laboratories, Livermore, CA 94551-9161, USA.

E-mail: emarqui@sandia.gov

Contract/grant sponsor: US Department of Energy; Contract/grant number: DE-F902-98ER45721.

were prepared by jet electropolishing with a solution of 5% perchloric acid in methanol at  $-30^{\circ}\text{C}$ . HREM was performed on a JEOL 4000EXII, at Argonne National Laboratory, at 200 kV to limit the amount of radiation damage produced by the electron beam. 3DAP microscopy tips with an end radius  $<50$  nm were obtained by a two-step electropolishing sequence on small rods of heat-treated material (10 mm long with a  $250\ \mu\text{m} \times 250\ \mu\text{m}$  cross-section). Initial electropolishing using a solution of 30% nitric acid in methanol was performed to shape the rods into long needles with a small taper angle. A solution of 2% perchloric acid in butoxyethanol was used for necking and final electropolishing to produce a sharply pointed tip. Analyses were performed at specimen temperatures below 30 K, at a background pressure of  $10^{-5}$  Torr consisting of a mixture of 80% Ne and 20% He for field ion microscopy imaging, and ultrahigh vacuum conditions ( $10^{-10}$  Torr) for pulsed field evaporation; evaporation was performed with a pulse fraction (pulse voltage/steady state d.c. voltage) of 20% and a pulse frequency of 1500 Hz.

### Data analysis

With respect to the mass-to-charge state ( $m/n_e$ ) spectrum, the three isotopes of Mg are doubly charged at 12, 12.5 and 13 amu with no hydride formation. Scandium is also doubly charged with multiple hydrides, showing a possible overlap between Sc and singly-charged Mg at  $m/n_e$  values of 24, 25 and 26 amu. In some cases, peaks at 24, 25 or 26 amu were detected, and the corresponding ions were considered to be Sc hydrides. One of the objectives of this study being the analysis of Mg concentrations, this choice limited overestimating the Mg concentrations, in particular in the proximity of the  $\text{Al}_3\text{Sc}$  precipitates. Most of the analyses were performed near a low-index crystallographic pole, and depth scaling of data sets was performed using the appropriate crystallographic interplanar spacing. Lateral scaling was deduced from a theoretical detection efficiency of 60% of the theoretical number density of atoms ( $60\ \text{atoms}\ \text{nm}^{-3}$  for Al). Data visualization and analysis of data sets were performed using the software program ADAM 1.5, which is described in Ref. 6. Values of composition are obtained by employing proximity histograms (or proxigrams for short), by reference to an interface, which display average concentrations in shells of thickness 0.4 nm at a given distance from an interface.<sup>7</sup> A cluster search algorithm was developed to detect clustering effects in the 3DAP microscope reconstructions, where clusters are defined by the maximum distance  $d$  between atoms.<sup>8</sup> Average radial concentration distributions around a given type of atom were also used to search for local ordering effects.

## RESULTS

3DAP observations were obtained for the as-quenched state and after aging at  $300^{\circ}\text{C}$  for 0.33, 0.5, 5 and 1040 h. These aging times correspond to critical stages of the precipitation process, as measured by Vickers microhardness (Fig. 1).

In the as-quenched state, the average composition is 2.26 at.% Mg and 0.17 at.% Sc. The statistical chi-squared

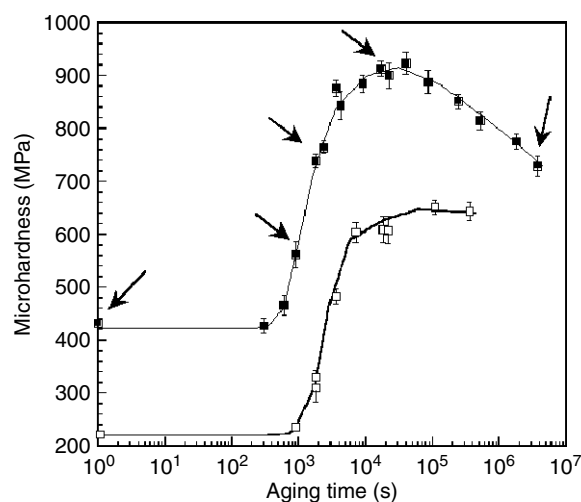


**Figure 1.** Vickers microhardness as a function of aging time at  $300^{\circ}\text{C}$  for Al-2 wt.% Mg-0.2 wt.% Sc (solid squares) and Al-0.2 wt.% Sc (open squares) alloys; the arrows indicate the heat treatments studied by 3DAP microscopy.

test, which compares solute concentration distributions with binomial distributions of a perfectly random solid solution, does not rule out whether or not Mg or Sc atoms are homogeneously distributed in the Al matrix. Magnesium radial concentration distributions around Mg atoms do not show any clustering effect. On the other hand, Sc radial concentration distributions around Sc atoms show a small enhancement for distances of  $<0.8$  nm, which corresponds to a significant number of pairs of Sc atoms detected using the cluster search algorithm, with a maximum separation distance of 0.5 nm. No strong correlations between positions of Mg and Sc atoms could be established.

After aging for 20 min, a small increase in hardness is measured (Fig. 1) and small precipitates with radii between 0.8 and 1.4 nm are observed by 3DAP microscopy. The estimated number density of precipitates, calculated from transmission electron micrographs, is  $4 \times 10^{22}$  precipitate  $\text{m}^{-3}$ . Eight precipitates were analyzed with an average composition of  $22.4 \pm 2.8$  at.% Sc, which is very close to the stoichiometric composition. Magnesium atoms are also present in the precipitates at a level of 4.3 at.%, which is slightly greater than the average concentration in the matrix. No Sc-rich clusters, other than Sc pairs, with sizes  $<0.8$  nm or of different compositions were detected using the cluster search algorithm.

After further aging, precipitate radii continue to increase from 1 nm after 30 min (Plate 1(a)) to 4.2 nm after 1040 h (Plate 1(b)), while the Sc concentration in the matrix decreases from 0.12 at.% after 0.33 h to 0.025 at.% after 1040 h. The morphology of the analyzed precipitates is approximately spheroidal, as can be seen from the 3DAP microscope reconstructions (Plate 1) and HREM observations (Fig. 2). Analyses of composition by the proximity histogram (Fig. 3) show that the width of the  $\alpha\text{-Al}/\text{Al}_3\text{Sc}$  interface is  $\sim 0.8\text{--}1.2$  nm. Similar to the observations obtained for shorter aging times, an enhancement of the Mg concentration is observed at the interface, with a peak concentration between 4.3 and 6.5 at.%

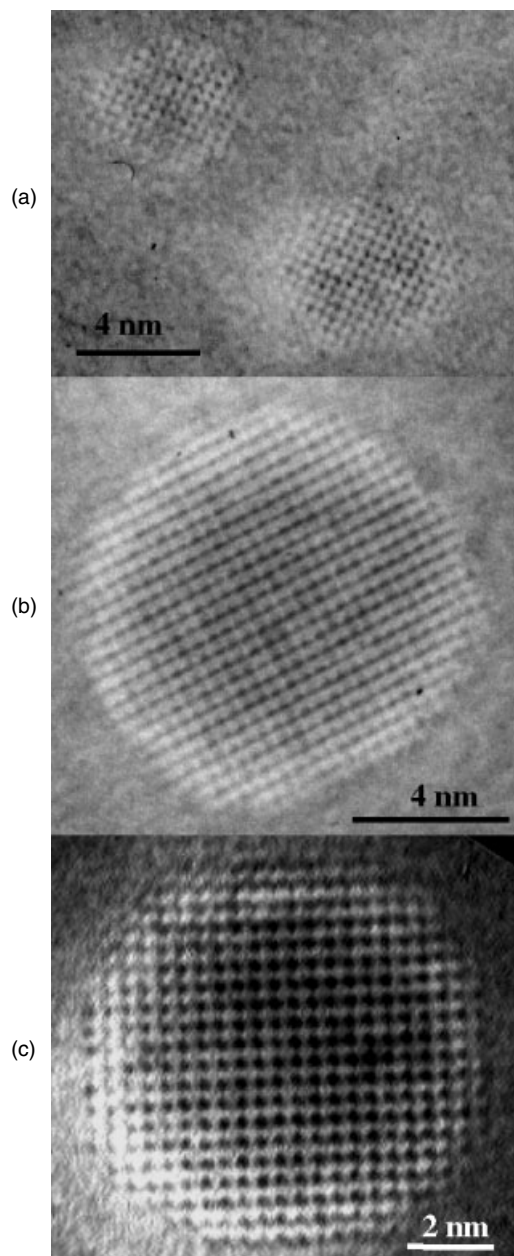


**Figure 2.** HREM ([100] zone axis) of Al<sub>3</sub>Sc precipitates in an Al–2 wt.% Mg–0.2 wt.% Sc alloy after aging at 300 °C for 30 min (a) and 1040 h (b); Figure 2(c) is an Al<sub>3</sub>Sc precipitate obtained in an Al–0.3 wt.% Sc alloy.<sup>16</sup> A small objective aperture selecting only the eight low-index superlattice reflections of the Al<sub>3</sub>Sc phase was used to form these images.

Mg. The proximity histogram represents concentration averages over all the crystallographic directions, and a possible orientation dependence of the Mg segregation behavior is not taken into account in this analysis. Magnesium atoms were also detected in the centers of the precipitates.

## DISCUSSION

### Precipitation

As the Al<sub>3</sub>Sc precipitates coarsen, the Sc concentration in the matrix decreases, as observed by 3DAP microscope analyses. This result is in agreement with the values

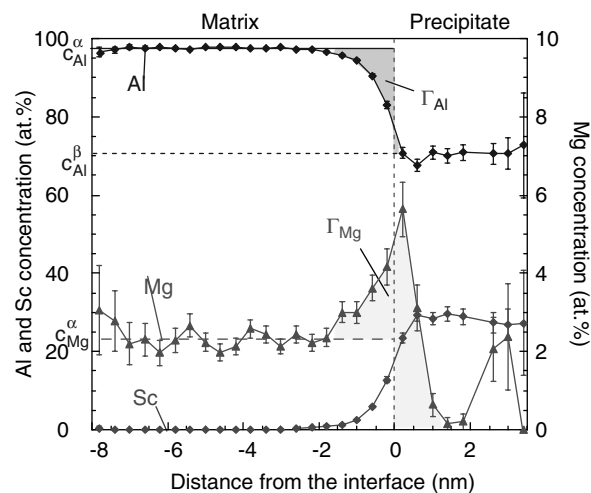


**Figure 3.** Proximity histogram of an Al<sub>3</sub>Sc precipitate after aging at 300 °C for 1040 h, showing Al, Mg and Sc concentrations with respect to the distance to the Al/Al<sub>3</sub>Sc interface. The Al, Mg and Sc Gibbsian excesses are indicated by the shaded areas.

obtained previously by Sano *et al.* for a binary Al–0.25 wt.% Sc alloy.<sup>9</sup> The Sc concentration measured after aging for 1040 h ( $(2.5 \pm 0.7) \times 10^{-2}$  at.%) is, however, higher than the value expected from thermodynamic data; that is, the Sc solid solubility in Al–2 wt.% Mg at 300 °C is  $6.1 \times 10^{-4}$  wt.% according to Joanne Murray (Alcoa Corp., personal communication). The composition of all the Al<sub>3</sub>Sc precipitates is close to the stoichiometric composition, even at the shortest aging times, and the variations in Sc concentration reported by Sano *et al.*<sup>9</sup> are not confirmed.

### Magnesium segregation at the Al/Al<sub>3</sub>Sc interface

The level of Mg segregation is quantified through the relative Gibbsian interfacial excess of Mg with respect to Al and Sc ( $\Gamma_{\text{Mg}}^{\text{relative}}$ ), which is independent of the locus of the interface and is defined by<sup>10</sup>

$$\Gamma_{\text{Mg}}^{\text{relative}} = \Gamma_{\text{Mg}} - \Gamma_{\text{Sc}} \frac{c_{\text{Al}}^{\alpha} c_{\text{Mg}}^{\beta} - c_{\text{Al}}^{\beta} c_{\text{Mg}}^{\alpha}}{c_{\text{Al}}^{\alpha} c_{\text{Sc}}^{\beta} - c_{\text{Al}}^{\beta} c_{\text{Sc}}^{\alpha}} - \Gamma_{\text{Al}} \frac{c_{\text{Mg}}^{\alpha} c_{\text{Sc}}^{\beta} - c_{\text{Mg}}^{\beta} c_{\text{Sc}}^{\alpha}}{c_{\text{Al}}^{\alpha} c_{\text{Sc}}^{\beta} - c_{\text{Al}}^{\beta} c_{\text{Sc}}^{\alpha}} \quad (1)$$

where  $\Gamma_{\text{Mg}}$  and  $\Gamma_{\text{Al}}$  are the Gibbsian interfacial excesses of Mg and Al and the  $c_j^i$  are the concentrations of component  $j$  ( $j = \text{Al}$  or  $\text{Mg}$ ) in phase  $i$  ( $i = \text{Al}$  or  $\text{Al}_3\text{Sc}$ ). Figure 3 illustrates the Gibbsian excess quantities for Al (negative value), Sc (positive value) and Mg (positive value) as the areas under the concentration curves in the proximity histogram.<sup>11</sup> The relative Gibbsian excesses of Mg with respect to Al and Sc are shown in Table 1 for the different aging times. The variation observed is within experimental error. The root-mean-squared diffusion distance of Mg in Al away from the precipitate interface, given by  $\sqrt{6Dt}$ , where  $D = 1.6 \times 10^{-16} \text{ m}^2 \text{ s}^{-1}$  is the diffusion coefficient of Mg in Al at 300 °C<sup>12</sup> and  $t$  is the aging time, is  $\sim 1.3 \mu\text{m}$  after 0.5 h of aging at 300 °C and  $60 \mu\text{m}$  after 1040 h. The precipitate spacing is evaluated using the square lattice spacing given

**Table 1.** Relative Gibbsian excess of Mg with respect to Al and maximum interfacial Mg concentration with respect to Al for different aging times

	Aging time			
	30 min	5 hours	300 hours	1040 hours
$\Gamma_{\text{Mg}}^{\text{relative}}$	$1.5 \pm 0.7$	$1.7 \pm 0.3$	$2.2 \pm 0.5$	$1.9 \pm 0.5$
$C_{\text{Mg}}^{\text{max}}/C_{\text{Mg}}^{\text{Matrix}}$	$2.8 \pm 0.3$	$2.0 \pm 0.2$	$2.3 \pm 0.5$	$1.9 \pm 0.4$

by  $r\sqrt[3]{4\pi/3f}$ , where  $r$  is the mean precipitate radius and  $f = 0.53$  vol.% is the calculated volume fraction of  $\text{Al}_3\text{Sc}$  precipitates at  $300^\circ\text{C}$ . The precipitate spacing is 10 nm for a mean precipitate radius of 1.1 nm (30 min of aging) and 39 nm for a mean precipitate radius of 4.2 nm (1040 h of aging). The root-mean-squared diffusion distance of Mg is therefore greater than the average interprecipitate spacing and the system is in global thermodynamic equilibrium with respect to Mg segregation at the  $\alpha\text{-Al}/\text{Al}_3\text{Sc}$  interface. The equilibrium state explains the similar values of the Gibbsian excess of Mg relative to Al and Sc for all aging times. The maximum value of concentration of Mg at the interface decreases after 0.5 h and remains constant for longer aging times (Table 1).

For a ternary alloy the classical thermodynamic Thomson–Freundlich equation<sup>13</sup> for the increase in solid solubility at an interface due to its curvature does not hold. The reason for this is that for steady-state diffusion-limited growth the equations governing the interface solute compositions are given by equations 6–8 in Kuehmann's and Voorhees' treatment of coarsening in a ternary alloy.<sup>14</sup> Note that the equality of chemical potentials (equation 7 of Ref. 14) gives only three equations, which is not sufficient to determine uniquely the four unknown compositions in a ternary alloy. The fourth condition comes from flux balance (mass conservation) at the moving precipitate/matrix interface, and the variation in solute concentrations with precipitate radius is affected not only by the interfacial free energy but also by the ratio of the solute diffusion parameters. For the Al–Sc–Mg system this treatment predicts a depletion of Mg at the  $\alpha\text{-Al}/\text{Al}_3\text{Sc}$  interface. Thus our observation of a positive value of the relative Gibbsian interfacial excess of Mg with respect to Al and Sc is further evidence that we are observing a thermodynamic equilibrium excess quantity.

The interesting aspect of these results comes from the coherency state of the matrix/precipitate interface. Several previous three-dimensional atom probe microscope studies reported the segregation behavior of solute atoms at partially semi-coherent or semi-coherent heterophase interfaces<sup>15</sup> but no experimental work has been reported on perfectly coherent heterophase interfaces. In the present study, the coherency state of the precipitate interface is known from HREM observations and was determined to be perfectly coherent for all cases presented. Coherency loss usually occurs when the precipitate size is large enough so that the spacing between the misfit dislocations is of the order of  $a/\delta$ , where  $\delta \sim 0.62\%$  is the lattice parameter misfit at  $300^\circ\text{C}$  between the Al matrix containing 2 wt.% Mg and the  $\text{Al}_3\text{Sc}$  phase, and  $a \sim 0.2$  nm is the spacing between {200}

planes. The critical precipitate diameter for coherency loss is  $\sim 30$  nm, which is much larger than the precipitate sizes observed after aging at  $300^\circ\text{C}$  for  $<1040$  h.

A consequence of Mg segregation at the interface is the change in morphology observed from faceted  $\text{Al}_3\text{Sc}$  precipitates parallel to the {100}, {110} and {111} planes in a binary Al–0.3 wt.% Sc alloy<sup>16</sup> to spheroidal precipitates in the presence of ternary Mg additions. The segregation behavior indicates a change in interfacial energy. In particular, as suggested by a Wulff plot, the reduction of the {100} facet length would correspond to a smaller decrease of {100} energy relative to an energy decrease of other crystallographic planes, leading to a more 'rounded' morphology.

The observed interface width may be explained by the artificially higher magnification of the precipitate. The exact shape of the precipitates observed by three-dimensional atom probe microscopy needs to be considered carefully, because it depends strongly on the field evaporation conditions and can be subject to significant experimental artifacts, e.g. asymmetry of the tip, misalignment of the analysis direction or different ionization behaviors of the matrix and the precipitate resulting in a smaller radius of curvature of the precipitate and thereby an artificially higher magnification of a precipitate with respect to the surrounding matrix, as suggested by the lower local atomic density of the  $\text{Al}_3\text{Sc}$  phase and its bright imaging behavior in a field ion microscope image.<sup>17</sup> The approximately spheroidal shape observed by HREM is, however, reproduced.

### Heterogeneous nucleation of $\text{Al}_3\text{Sc}$ ?

Besides peaks of Mg concentration at the interface, an enrichment of Mg atoms inside the  $\text{Al}_3\text{Sc}$  precipitates is observed. In particular, after 1040 h of aging the precipitate cores contain 15–42 Mg atoms. It is speculated that  $\text{Al}_3\text{Sc}$  precipitation occurs as a result of interactions between Mg and Sc atoms with vacancies, which leads to a faster nucleation rate than in the binary Al–Sc alloy, as demonstrated by the microhardness measurements (Fig. 1). The high concentration of quenched-in vacancies and their high mobility, even at room temperature, could explain the fairly high number of Mg–Sc dimers and, during the formation of a stable nucleus involving the Mg–Sc dimers, Mg atoms may become trapped within the small growing  $\text{Al}_3\text{Sc}$  precipitates as Sc diffuses to the precipitates. No data on diffusion of any element in  $\text{Al}_3\text{Sc}$  could be found in the literature. It is possible that magnesium is not able to diffuse through the  $\text{Al}_3\text{Sc}$  phase to the matrix, which would explain the shape of the Mg concentration profile observed in Fig. 3, even though the equilibrium ternary Al–Mg–Sc phase diagram does not predict any Mg solubility in the  $\text{Al}_3\text{Sc}$  phase.

### CONCLUSIONS

Three-dimensional atom probe microscopy analyses performed on Al–2 wt.% Mg–0.2 wt.% Sc alloys aged at  $300^\circ\text{C}$  for various times leads to the following results:

- (1) The  $\text{Al}_3\text{Sc}$  precipitates form with stoichiometric composition and include  $\sim 4.3$  at.% Mg.

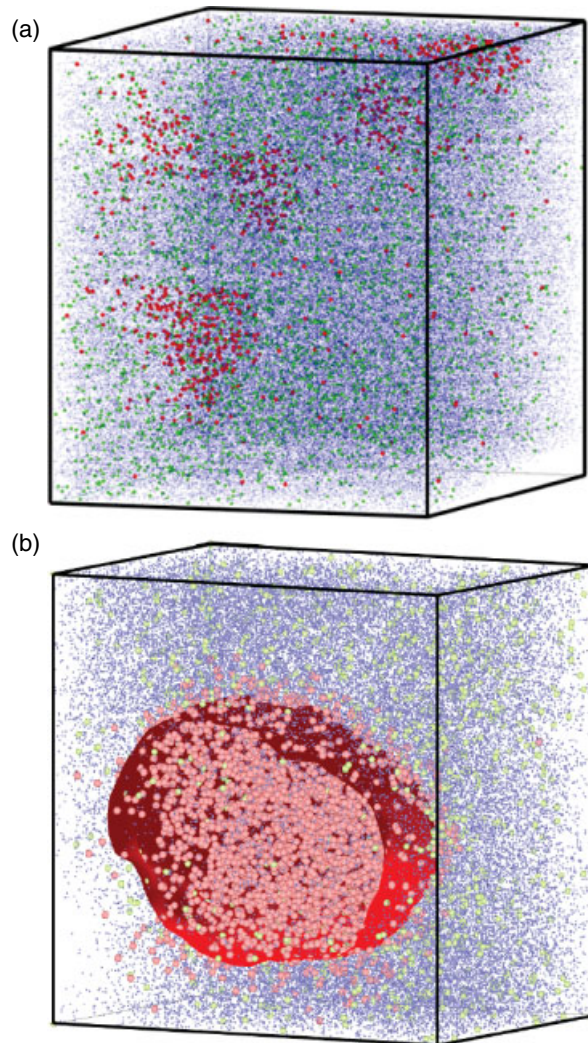


**Plate 1.** 3DAP reconstruction of an analyzed volume from a tip aged at 300 °C: (a) for 5 h, displaying Sc atoms, with box dimensions of 24 nm × 23 nm × 27 nm; (b) for 1040 h, with box dimensions of 17 nm × 18 nm × 8 nm. (Sc atoms are in red, Mg atoms in green and Al atoms in blue).

- (2) The mean precipitate radius increases from 0.8 to 4.2 nm when aged from 20 min to 1040 h.
- (3) An enhancement of the Mg concentration by a factor of 2–3 at the matrix/precipitate interface is measured for all aging times. Segregation is occurring at the perfectly coherent  $\alpha$ -Al/Al<sub>3</sub>Sc interface, whose structure has been determined from an HREM study. This thermodynamic equilibrium Mg segregation behavior corresponds to a relative Gibbsian excess of Mg with respect to Al and Sc of 1.9 atoms nm<sup>-2</sup> and is the source of the change in precipitate morphology, e.g. the disappearance of the {100} facets.
- (4) Magnesium is observed at the center of the Al<sub>3</sub>Sc precipitates and may be attributed to attractive interactions between Sc and Mg atoms during the early stages of Al<sub>3</sub>Sc precipitation, which would also explain the faster nucleation behavior of the Al–Mg–Sc alloy compared with a binary Al–Sc alloy.

### Acknowledgements

This research is supported by the United States Department of Energy, Basic Sciences Division, under contract DE-FG02-98ER45721. The authors thank Professors Mark Asta and David Dunand (Northwestern University) for very interesting discussions.

### REFERENCES

1. Toporova LS, Eskin DG, Kharakterova ML, Dobatkina TB. *Advanced Aluminum Alloys Containing Scandium*. Gordon & Breach: Amsterdam, 1998.
2. Marquis EA, Seidman DN, Dunand DC. *Acta Mater.* 2002; **50**: 4021; erratum 2002; **51**: 285.
3. Hatch JE. *Aluminum: Properties and Physical Metallurgy*. ASM: Metals Park, OH 1984.
4. Ringer SP, Hono K. *Mater. Charact.* 2000; **44**: 101.
5. Asta M, Ozolins V, Woodward C. *JOM* 2001; **53**: 16.
6. Hellman O, Vandenbroucke J, Blatz du Rivage JB, Seidman DN. *Mat. Sci. Eng. A* 2001; **327**: 29.
7. Hellman OC, Vandenbroucke JA, Ruesing J, Isheim D, Seidman DN. *Microsc. Microanal.* 2000; **6**: 437.
8. Kluthe C, Al-Kassab T, Kirchheim R. *Mater. Sci. Eng. A* 2002; **327**: 70.
9. Sano N, Hasegawa Y, Hono K. *J. Phys. Suppl.* 1987; **C6-48**: 337.
10. Dregia SA, Wynblatt P. *Acta Metall. Mater.* 1991; **39**: 771.
11. Krakauer BW, Seidman DN. *Phys. Rev. B* 1993; **48**: 6724.
12. Rothman SJ, Peterson NL, Nowicki LJ, Robinson LC. *Phys. Status. Solidi. B* 1974; **63**: K29.
13. Swalin RA. *Thermodynamics of Solids*. John Wiley & Sons: New York, 1972; p. 183.
14. Kuehmann CJ, Voorhees PW. *Metall. Mater. Trans. A* 1996; **27**: 937.
15. Isheim D, Hellman OC, Seidman DN, Danoix F, Blavette D. *Scr. Mater.* 2000; **42**: 645.
16. Marquis EA, Seidman DN. *Acta Mater.* 2001; **49**: 1909.
17. Vurpillot F, Bostel A, Blavette D. *Appl. Phys. Lett.* 2000; **76**: 3127.